Influence of drilling and abrasive water jet induced damage on the performance of carbon fabric/epoxy plates with holes

John Montesano [a], Habiba Bougherara [b] and Zouheir Fawaz [c]

[a] Mechanical and Mechatronics Engineering, University of Waterloo, Waterloo, ON N2L 3G1, Canada
[b] Mechanical and Industrial Engineering, Ryerson University, Toronto, ON M5B 2K3, Canada
[c] Aerospace Engineering, Ryerson University, Toronto, ON M5B 2K3, Canada

Corresponding Author: John Montesano, Email: john.montesano@uwaterloo.ca, Tel: 1(519)888-4567, ext. 38086

Abstract

The influence of conventional drilling (CD) and abrasive water jet (AWJ) cutting on the fatigue performance of carbon fabric/epoxy plates was investigated. Observations of machined hole regions revealed more severe damage on the CD hole surfaces with larger damage regions penetrating into the material. For both material systems investigated, the surface roughness for AWJ holes was in fact higher in comparison to CD holes. Nonetheless, static properties, short-term fatigue properties and endurance limits of the plates were not affected by the machining technique. Observed damage, stiffness and temperature evolutions during short-duration cyclic tests showed no significant changes in fatigue response for CD and AWJ plates, suggesting that surface roughness is not a good indicator of hole quality. However, long-duration cyclic tests revealed that CD plates exhibited greater stiffness degradation and advanced damage after a cyclic threshold, beyond which machining-induced delamination cracks began to propagate. This was not observed for the AWJ plates, where instead cyclic loading-induced delamination cracks initiated and propagated much later. These key findings are critical for assessing the unique performance characteristics of fabric/epoxy plates with holes. Since these materials are increasingly used for primary fatigue-critical structures, the presented outcomes are vital for designing corresponding structure joining methods.

Keywords: Fabric carbon fiber/epoxy; fatigue; thermography; water jet; drilling; damage

1. Introduction

The superior fatigue performance and versatility of carbon fiber reinforced plastics (CFRP) have made them favourable for several structural applications, including automobile chassis and aircraft wing components, where they are replacing conventional metallic alloys. More specifically, fabric CFRPs are now increasingly being used for primary load-bearing structures requiring adequate in-plane mechanical performance and improved out-of-plane strength [1]. However, their intricate microstructure presents many challenges when compared to laminated CFRPs with unidirectional plies, including the assessment of their microscopic damage processes and the resulting material property degradation. These are important material characteristics for fatigue critical structural components, where long-term durability is paramount. In structural applications, holes are often machined in order to assemble fabric CFRP parts with other components. Thus, the long-term performance of these components hinges on the quality and accuracy of the machined holes [2].

Conventional drilling (CD) using twist drills is commonly utilized in the automotive and aircraft industry for producing holes in fiber reinforced composite parts [3]. A number of studies have reported various damage modes resulting from various drilling process in composite laminates or chopped mats [4–21]. The severity of hole drilling induced damage is mainly influenced by the choice of machining parameters, the tool geometry, and the specific properties of the composite material. One of the most common forms of drilling damage is delamination at the exit plane, which is caused by the thrust force exerted by the drill cutting edge as it exits the composite laminate material. Kilickap [12, 13] and Mohan et al. [7], among others, concluded that higher feed rates and cutting speeds had greater influence on the delamination severity and

thrust force, while Singh et al. [9] found that the thrust force increased with increasing drill point angle. Other common forms of hole drilling damage includes defects on the hole surface, such as cracks and cavities in matrix rich regions, matrix degradation and fiber pull-out, which all result in notable surface roughness. Khashaba [22] and Khan et al. [17] reported that matrix materials with lower thermal properties produced higher temperature rises around holes during drilling, which resulted in matrix degradation on the hole surface. Manna et al. [10] found that the cutting speed and the feed rate were also the main machining parameters that influence the hole surface roughness.

The hole drilling damage arising from CD processes can have a major impact on the mechanical properties of composite parts. Persson et al. [2] investigated the drilling defects around holes in carbon/epoxy multidirectional laminates using various drilling techniques. They concluded that holes containing more damage (i.e., higher surface roughness) had significantly lower compressive and bearing strengths, and notably lower fatigue lives. Khashaba et al. [23] also found that woven glass/epoxy composites with drilled holes containing more damage resulted in notably lower bearing strengths. Saleem et al. [24] studied the effects of different machining processes on the hole surface quality of angle-ply CFRP laminates. They found that holes with fewer visible surface defects did not affect the static tensile strength of the laminates; however, the fatigue strength was notably reduced.

In order to minimize the defects associated with machining holes in composite parts, a non-traditional machining technique using an abrasive water jet (AWJ) has been utilized in recent years. AWJ machining is an alternate method that is now widely used for cutting composite materials, which does not produce a heat-affected zone during the cutting process and does not cause workpiece distortion. The effect of AWJ process parameters on the cut surface quality of

glass or carbon fiber/epoxy composites have been recently investigated [25, 26], where abrasive size and type, operating pressure and transverse feed rate have been observed to have the most influence. Comparisons between the cut surface quality of AWJ and conventional machining processes and their effects on mechanical performance of multidirectional CFRP laminates were recently reported [24, 27, 28].

These previously reported studies that have correlated the performance of GFRPs and CFRPs with the machined hole surface quality have made notable contributions to this field. However, it is clear that these studies focussed on the performance of laminates constructed from unidirectional plies. Few studies consider fabric-reinforced polymer composites in general, where to the knowledge of the authors a comparative study focused on the performance of fabric CFRPs have not yet been investigated. The particular fiber architecture will undoubtedly impact the hole surface quality, the associated machining induced damage modes, and the overall performance. The goal of this study is to investigate the influence of CD and AWJ machining process on the fatigue performance of two types of woven CFRP composite plates with holes through a comprehensive experimental program. The paper describes details of the CD and AWJ machining processes used on the woven CFRP composite plates, and the associated hole surface quality analysis. Details of the conducted static and fatigue tests are also presented, which aim to analyze damage evolution, stiffness degradation and thermal dissipation via various infrared thermographic (IRT) methods. The authors believe that the uniqueness of this study stems, among other factors, from its focus on fabric CFRPs and the use of novel non-destructive evaluation methods to observe fatigue damage evolution as a function of the two distinct machining methods.

2. Materials and Experimental Methods

2.1 Woven CFRP Materials and Machining Details

Two distinct woven CFRP materials were considered in this study. The first was AGP370-5H/3501-6S, which is a five-harness satin (5HS) woven carbon fabric/epoxy composite supplied in prepreg form. The fiber yarns consisted of 6,000 AS4 carbon fibers with the same tow count in both the warp and weft directions. The second material was SGP370-8H/8552, an eight-harness satin (8HS) woven carbon fiber fabric/epoxy composite also supplied in prepreg form, with fiber yarns consisting of 6,000 IM7 carbon fibers and the same tow count in warp and weft directions. For each material, flat plates were manufactured by stacking 7 layers of the corresponding prepreg fabric with the same orientation, producing final plate thicknesses of 2.7 mm. Test coupons with nominal dimensions of 32 mm × 255 mm were cut from these plates along the woven fabric warp direction, in accordance with ASTM D5766. Thereafter, holes with a diameter of ∅5.1 ± 0.04 mm were cut at the center of each test coupon using either AWJ or CD as described in the subsequent paragraphs. The chosen hole diameter is commonly used for many aerospace applications requiring mechanical fasteners such as rivets, bolts or locking pins, while the thickness is also typical for many structural applications. The coupon width is also based on the recommendation from ASTM D5766 (i.e., 32 mm > 6 x 5.1 mm). Studies of conventional drilled FRP laminates [7, 15, 29] have shown that larger plate thicknesses and hole diameters increase the thrust force, which may affect the associated hole quality and part performance. In the study by Ibraheem *et al.* [30] using AWJ to produce holes in GFRP plates, it was reported that thicker plates exhibited slightly lower ultimate tensile strengths. The effects of plate thickness and hole diameter not been investigated in this study and is beyond the scope;

however, it should be noted that a study on fabric CFRPs comparing the effects of hole diameter and panel thickness using different drilling methods on performance has not been reported.

For the first set of test coupons, an AWJ method was utilized to cut holes in both the 5HS and 8HS CFRP test coupons. The abrasive size and jet incident angle were fixed at 177 μm (i.e., 80 mesh) and 90°, respectively, which were limitations of the available AWJ machine. Note that a preliminary analysis was conducted whereby the standoff distance and jet pressure were varied in order to determine the effects on the hole surface roughness. It was found that higher pressures and smaller standoff distances led to optimal surface qualities, which was in agreement with reported findings [31]. The final process parameters used were a standoff distance of 1.5 mm and a pressure of 380 MPa (i.e., the maximum capable of the available AWJ machine), which resulted in reference hole surface roughness values presented in the results section.

For the second set of test coupons, a CD technique using uncoated brad-point carbide drill bits was used to drill the holes in the 5HS and 8HS CFRP test coupons. Note that the drill bits used in this study were not previously used, and that there was no indication of any notable tool wear (fewer than 20 holes were drilled with each bit). This was done to eliminate tool wear as a potential damage source [11] and, therefore, as a focus of the study. Also, the drill bit geometry and type was not considered in this study, however, it should be noted that this may have an effect on the drilling thrust force and exit plane delamination [32, 15, 19]. Another preliminary analysis was conducted in order to determine the spindle speeds and feed rates required to produce similar hole surface roughness profiles as produced by AWJ. Various combinations of spindle speed and feed rate were tested for this purpose using a numerically controlled (NC) drill press. The final machining parameters used were a spindle speed of 1000 rpm and a feed rate of 0.125 mm/rev (see results section for corresponding surface roughness values).

The final machining parameters chosen for the AWJ and CD techniques allowed for a one-to-one comparison between the performance of the corresponding test coupons. In order to analyze the resulting test coupon hole surface quality, a profilometer was used to measure the average surface roughness (*Ra*), the average distance between highest peak and lowest valley (*Rz*), and the quadratic mean surface roughness (*Rq*) in both the circumferential and through-thickness directions of the hole surfaces. A plate thickness of 2.7 mm provided an adequate distance to measure the roughness values along the through-thickness direction with the profilometer, as has been performed for plates with similar thicknesses [24]. Note that *Ra*, *Rz*, and *Rq* values were measured in order to determine if either of these parameters are good indicators of the machined surface quality for CFRPs, which has been previously investigated for CFRP laminates [33]. In addition, optical and scanning electron microscopes (SEM) were used to visualize surface characteristics.

This manufacturing process resulted in four sets of test coupons, which are listed in Table 1. All test coupons were equipped with 10° tapered aluminum end tabs in order to minimize potential issues with gripping induced failure, which is in accordance with ASTM D5766. The test coupon geometry is shown in Fig. 1.

2.2 Experimental details

All in-plane uniaxial tensile static and fatigue tests were conducted at room temperature on an MTS 322 test frame equipped with hydraulic wedge grips. A surface mounted extensometer was used to monitor the axial strain and for calculation of the degrading material stiffness during the cyclic loading tests, and was positioned with its knife edges about the hole (see Fig. 1). A FLIR SC5000 infrared camera with a 320 × 240 pixel resolution and a temperature sensitivity of

<20 mK, which was synchronized to the test controller, was used to monitor the test coupon surface temperature during loading. Note that the emissivity for the tested CFRP materials was assumed to be 1.0 based on reported studies [34].

Three types of tests were performed in this study: (i) static, (ii) fatigue, and (iii) stepwise fatigue. Ultimate static tensile tests were conducted in displacement control with a constant crosshead speed of 1.2 mm/min, in accordance with ASTM D5766. These quasi-static tests were conducted for each of the four sets of test coupons in order to obtain the associated ultimate tensile strengths and stress-strain curves. In addition, tension-tension fatigue tests were conducted in load control using a constant amplitude sinusoidal waveform, a loading frequency of 10 Hz, and a stress ratio of 0.1 at maximum applied stress levels of 85% and 95% UTS, in accordance with ASTM D7615. The fatigue tests were conducted for a pre-defined number of stress reversals. These tests were conducted at high stress levels for each set of test coupons in order to track degradation of the material axial stiffness and thermal dissipation. Finally, stepwise tension-tension cyclic tests were conducted in load control using a loading frequency of 10 Hz, a stress ratio of 0.1, and variable peak stress amplitudes. The test coupons were subjected to loads with maximum stresses ranging from 30% UTS to 90% UTS, each for blocks of 7,000 cycles, and were conducted for each of the four sets of test coupons. The main goal was to rapidly evaluate the fatigue endurance limit using the collected temperature data, in lieu of a conventional and costly Wohler (*S*-*N*) curve approach. For additional details of this stepwise thermographic approach, the reader is referred to the literature [35, 36].

3. Results and Discussion

Prior to conducting the experimental test program, a quality analysis of the manufactured hole surfaces for all four sets of test coupons was conducted. The aim was to investigate the different types of damage modes on the hole surfaces, as well as the depth of damage penetration into the material. These details for the tested coupons are first discussed, while results for the static and fatigue tests are subsequently presented.

3.1 Surface quality and damage assessment

Sample plates containing CD and AWJ holes were used for this assessment. These were sectioned after cutting to allow for visual inspection of the hole surfaces using an optical microscope and an SEM. The AWJ hole surfaces in both the 5HS and 8HS CFRPs were characterized by streaks and craters oriented along the direction of the jet axis (see Fig. 2(a)), which are attributed to the abrasive particles in the jet stream. These damage modes were local to the matrix, were not accompanied by matrix fallout or fiber pullout, did not penetrate into the material, and were uniformly distributed on the entire hole surfaces in both the warp and weft yarns. For samples with drilled holes (CD), both the 5HS and 8HS CFRPs contained regions of cavities associated with fiber pullout and matrix fallout (see Fig. 2(b)), which resulted from the relative angle between the cutting tool edge direction and the fiber orientation. These damage modes were non-uniformly distributed around the hole surface (i.e., they were observed in some regions and not in others); however, they were mainly observed in the weft yarns. Exit plane delamination was also observed for most holes machined using the CD method (see Fig. 2(b)), which resulted from the thrust force of the drill as it passed through the panel. Although most CD holes exhibited exit plane delamination for both the 5HS and 8HS coupons, the source of this inconsistency is not known since the drilling parameters were kept constant, and as previously

indicated the tool wear was found to be negligible. One explanation may be the possibility of slight fiber misalignment resulting from processing of the woven CFRP plates, which may have an impact on exit plane delamination formation. It should be noted that all holes machined using the AWJ technique did not exhibit any delamination.

Surface roughness measurements for the machined holes were taken using a profilometer with a stylus. The average *Ra*, *Rq*, and *Rz* values for the 5HS and 8HS materials are listed in Table 2, for both AWJ and CD holes. Note that the variations of all the tabulated data points are within ±7%. For the drilled hole surfaces, the roughness values were approximately 15 – 25% higher for the 5HS material. This can be attributed to larger fiber yarns in the 5HS material promoting larger regions of matrix fallout during drilling when compared to the 8HS material. For the AWJ holes, the surface roughness values are consistent for both the 5HS and 8HS materials (i.e., the abrasive behaviour is consistent regardless of the fiber architecture). The surface roughness parameters were also higher for the AWJ holes as shown, which is a function of the final machining parameters. Note that the *Rz* values are notably higher than the *Ra* and *Rq* values for all cases, which is consistent with findings for CFRP laminates [33]. Although the roughness values are similar in magnitude for the AWJ and CD hole surfaces, the observed damage modes were dependent on the specific machining process. Thus, using a surface roughness criterion (i.e., *Ra*, *Rq* or *Rz*) alone for quantifying the quality of machined holes is not suitable for CFRPs. This is in line with observations made by Saleem et al. [24] for angle-ply CFRP laminates.

One important point is that surface roughness measurements do not adequately capture the total depth of sub-surface damage penetration within the CFRP material. From Fig. 2, it is clear that for the drilled holes, exit plane delamination and matrix cracks penetrated into the material

from the hole surface. To assess this, a pulsed thermographic (PT) technique was used to map the damage zone around machined holes in each of the four types of test coupons. PT is a widely used thermographic technique in the aerospace industry for inspecting defects in composite parts [37]. The samples were thermally stimulated using pulse heating for a short time period of 5 seconds using lamps with quartz bulbs, and the resulting thermal transients were captured with the FLIR SC5000 infrared camera with a rate of 50 Hz. The 5 second time period allowed for adequate heating of the coupons to produce measurable temperature transients. During cooling, the damaged regions dissipate heat at faster rate when compared to the non-damaged regions, and as a result the local temperatures will be higher in these regions. In this study, the samples were coated with mat black paint in order to minimize the effect of reflected infrared waves on the CFRP material, which provided improved thermographic image quality. Captured thermographs for 8HS-CD and 8HS-AWJ test coupons are shown in Fig. 3, where the thermal maps denote temperature changes and the drilled holes can be seen as darker regions (i.e., low temperature) at the test coupon centers. The AWJ test coupons showed very limited damage penetration into the material, which is evident by the thin bright region (i.e., high temperature) in Fig. 3(a). The streaks and craters caused by the abrasive particles were only observed on the hole surfaces. On the other hand, CD test coupons show a larger damage region around the hole resulting from localized delamination cracks penetrating into the material at the drill exit plane and matrix cracks penetrating from the hole surface. Note that the observed damage did not penetrate the material more than 2 mm from the drilled hole surface for all coupons investigated, and was not uniform around the hole periphery (see Fig. 3(b)). Similar observations were made for the 5HS-CD and 5HS-AWJ coupons, and there was no distinct difference in the delamination zone size and contour for the 5HS-CD and 8HS-CD coupons.

3.2 Static results

Representative ultimate tensile static stress-strain curves for the four sets of test coupons are shown in Fig. 4 – a total of 4 tests were conducted for each type of test coupon. Each curve is characterized by two distinct regions. In the first region there is linear stress-strain behaviour with a constant axial modulus, whereas in the second region there is slight nonlinear behaviour prior to failure. This nonlinear deformational response results mainly from elongation of the hole which is captured by the surface mounted extensometer, as well as the accumulation of microscopic cracks in the weft yarns [38] that leads to a non-uniform reduction in the local stiffness in the hole vicinity. For all test coupons, fracture occurred suddenly through a transverse plane in the hole vicinity, where the fracture regions were localized and brittle in appearance. The average ultimate tensile strength and axial stiffness for all 8HS test coupons were 550 MPa ± 4% and 59.25 GPa ± 5%, respectively, and similarly for all 5HS test coupons these values were, respectively, 409 MPa ± 3% and 48.3 GPa ± 2%. The 8HS composite has a higher strength and stiffness when compared to the 5HS, which is due to the particular woven fiber architecture. The 8HS CFRPs have fewer interlacing points, and thus less process-induced fiber crimping, which results in a much stiffer response under tensile loading.

It is evident from the plots in Fig. 4 that the hole machining technique (CD or AWJ) has no effect on the static behaviour of both the 5HS and 8HS woven CFRP materials. This is in spite of significantly more machining-induced damage observed in the CD coupons (i.e., matrix craters/fallout, fiber pullout and localized delamination), or higher surface roughness measurements for the AWJ coupons. Montesano et al. [38] reported that during static tensile loading, the main evolving damage mechanism observed in the 5HS and 8HS CFRPs was weft

yarn matrix cracking; however, these cracks were not induced during the machining of either the CD or AWJ coupons. Thus, during static loading the machining-induced damage around the hole did not notably propagate, whereas weft yarn cracks initiated and propagated instead which explains the null effect of the machining method.

3.3 Fatigue results

Stepwise cyclic tests were conducted where the overall temperature rise, ΔT, attained after $N^* = 5{,}000$ applied loading cycles (i.e., stress reversals) for a particular maximum applied cyclic stress was captured using the infrared camera. This was repeated for various maximum applied cyclic stresses for each individual test coupon. Characteristic bilinear plots of $\Delta T / N^*$ as a function of maximum applied cyclic stress are shown respectively in Figs. 5 and 6 for 5HS and 8HS CFRP test coupons, where the intersection of the lines on each plot correspond to the component fatigue endurance limit. The average endurance limit for the 5HS-AWJ coupons was 259 MPa ± 4 MPa, while the average value was 261 MPa ± 5 MPa for the 5HS-CD coupons. As can be seen, the endurance limit for the AWJ and CD coupons is statistically the same. This implies that the additional damage mechanisms observed in the vicinity of the hole of the CD coupons did not have an impact on the fatigue endurance limit. Similarly, for the 8HS-AWJ and 8HS-CD, the average endurance limits were found to be 355 MPa ± 3 MPa and 356 MPa ± 5 MPa, respectively. These results clearly show that the machining process does not seem to greatly affect the fatigue performance of the 5HS and 8HS woven CFRP materials. This is contrary to the results reported by Saleem et al. [24] for angle-ply CFRP laminates, where test coupons machined using AWJ had endurance limits 10% greater than the coupons machined by CD.

The temperature evolution and normalized stiffness degradation captured during 50% and 90% UTS maximum stress cyclic segments for 5HS-CD and 5HS-AWJ test coupons are shown in Fig. 7, which are representative of all tested coupons. When the 5HS woven CFRP is cycled with a maximum stress below the endurance limit, the stiffness and temperature profiles are virtually the same regardless of the machining technique used. Once the maximum stress in the stepwise loading sequence exceeds the endurance limit, the stiffness degradation and associated temperature rise is slightly higher for the CD test coupons. From Figs. 7(a) and (b), the stiffness degradation and temperature rise are respectively 1% and 4% greater for the CD coupons, which is a relatively minor increase. Similar results were obtained for the 8HS test coupons, as shown in Figs. 7(c) and (d). At lower stresses (i.e., below the endurance limit) the 5HS and 8HS woven CFRP plates did not exhibit significant damage evolution, where the main damage mechanism was cracking in the weft yarns, which is consistent with reported observations [38]. As a result, machining-induced damage around the holes did not propagate at lower cyclic stresses. At higher cyclic stresses, again the main damage mechanism in the CFRP plates was cracking in the weft yarns. Therefore, it can be gleaned that during short-term cyclic tests the hole machining technique does not influence the fatigue performance of the woven CFRP plates.

In order to investigate the long-term durability of the 5HS and 8HS woven CFRP plates, conventional tension-tension fatigue tests were conducted under high-stress cyclic loading. The corresponding normalized stiffness and temperature profiles are illustrated in Fig. 8 for 8HS-AWJ and 8HS-CD test coupons that were cycled with a maximum stress of 530 MPa. The stiffness and temperature data for both test coupons correspond well up to approximately 60,000 loading cycles, which further confirms that the short-term fatigue performance is not influenced by the hole machining technique (CD or AWJ). However, once the number of loading cycles

increases beyond this threshold, the stiffness and temperature data begins to deviate as shown in Fig. 8. It is clear that the plate machined by the CD process exhibits greater temperature rise and stiffness degradation when compared to the plates machined with the AWJ technique. After 100,000 cycles, the 8HS-CD test coupon exhibited an additional 3% drop in stiffness and 30% higher temperature rise, which corresponds to an advanced damage state. After 200,000 loading cycles, an additional 8% drop in stiffness and a 78% higher temperature rise was detected in the 8HS-CD test coupon, which is a significant deviation.

Clearly, the hole machining technique has a direct influence on the long-term fatigue performance of the woven CFRPs. In order to assess the damage zone size around the machined holes of the tested coupons, the same PT technique described previously was used. Acquired thermographic images for 5HS-AWJ and 5HS-CD coupons after 200,000 load cycles under a maximum stress of 385 MPa are shown in Fig. 9. The fatigued AWJ coupons did not exhibit notably larger damage zones (compare Figs. 9(a) and 3(a)), which shows that inter-ply delamination cracking was limited until this stage. On the other hand, the fatigued CD coupons exhibited notably larger damage zones after 200,000 cycle (see Fig. 9(b)), which corresponds to an advanced delamination region. Montesano et al. [38] reported that cyclically loaded 5HS and 8HS CFRPs exhibited three distinct stages of damage evolution. During the first stage weft yarn cracking initiated and multiplied, causing rapid stiffness degradation, which eventually saturated. This signified the onset of the second stage where localized intra-ply yarn interface cracks initiated, which was followed by the final stage involving delamination crack growth and crack interaction. In this study, the AWJ test coupons follow the same three-stage damage progression during cyclic loading in the regions near the central hole. However, the CD coupons exhibit delamination cracking much sooner, which results from the machining induced damage at the

hole surface. From Fig. 3(b), the depth penetration of the drilling induced damage is limited to the length of the local cut yarns. It seems that up until the loading cycle threshold, the machining induced delamination does not propagate since it is effectively arrested by these yarns in the CD coupons. After the loading cycle threshold is exceeded, there is enough energy to cause these localized machining induced delamination cracks to grow. As mentioned, this occurs much sooner for the CD coupons in comparison to the AWJ coupons, which do not exhibit delamination until much later during cycling (i.e., during the final cyclic stage). Therefore, for the studied woven CFRP materials, the influence of the machined hole technique on the long-term fatigue behaviour at high applied stresses is mainly due to the existence of delamination for the drilled coupons. Although not studied here, the size of the drilling induced delamination will likely also be a factor under these loading conditions. It should be noted that both the 5HS and 8HS woven CFRP plates exhibited the same damage characteristics.

4. Summary of observations

First, the machining induced damage on the hole surface for CD and AWJ test coupons was assessed. It was found that the measured surface roughness values (i.e., *Ra*, *Rq*, *Rz*) for the drilled holes were slightly lower for the 8HS material. This is a result of the smaller fiber yarns promoting smaller matrix fallout regions, which demonstrates that drilling-induced damage in CFRPs is dependent on fiber architecture. The AWJ holes exhibited the same roughness values for both CFRP materials, which shows that fiber architecture does not influence the hole surface quality resulting from water jet particle abrasion. In addition, the surface roughness parameters for the AWJ holes were higher when compared to the CD holes for both CFRP materials

considered. Subsequent scanning electron microscopy revealed that the CD test coupons had severe damage modes, including localized delamination at the hole exit plane, and fiber pullout and matrix fallout within the weft yarns. In contrast, the AWJ coupons exhibited narrow streaks and craters aligned with the jet direction, which were uniformly distributed around the hole surface. Comparison of the *Rz* values for CD and AWJ holes infers that the streaks on the AWJ hole surfaces are deeper than the matrix fallout craters observed on the drilled hole surfaces. Also, a pulsed thermographic technique was used to detect and map the depth penetration of damage around the machined holes, which revealed that the CD coupons had notably larger damage zones penetrating much farther into the material from the hole surfaces. Thus, although the magnitude of the surface roughness parameters for the AWJ holes were greater than for the drilled holes, the surface roughness alone is not a good indicator of the hole quality for fabric CFRP materials, which is a significant finding.

Next, tensile static and fatigue tests were conducted for the woven CFRP materials, for CD and AWJ test coupons. The static performance for both 5HS and 8HS woven CFRPs were not influenced by the hole machining technique used, where the same ultimate strength was obtained for both CD and AWJ coupons. The main evolving damage mechanisms during static loading were weft yarn cracks, whereas the observed machining induced damage did not propagate during static loading, which explains the null effect of the machining process. During stepwise cyclic tests, the fatigue endurance limit was evaluated using a thermographic technique for 5HS and 8HS woven CFRP coupons. It was found that the hole machining technique (CD or AWJ) did not influence the magnitude of the endurance limit, and that the short-term durability of the woven CFRP plates was also not influenced as was assessed by monitoring stiffness degradation and temperature rise profiles during stepwise cyclic tests. This is due to the lower notch

sensitivity of fabric CFRPs, and differs from the results reported in other studies conducted on unidirectional ply CFRP laminates.

In contrast, the long-term fatigue performance of both the 5HS and 8HS woven CFRP plates was significantly influenced by the machining technique used to machine the round holes. Conventional tension-tension fatigue tests under high applied stress (i.e., > 90% UTS) cyclic loading revealed that up to a certain cyclic interval, the CD and AWJ coupons exhibited the same stiffness degradation, temperature profiles, and damage evolution characteristics. However, beyond this cyclic threshold the CD coupons exhibited greater stiffness degradation and temperature rise, which was correlated to growing delamination cracks in the hole vicinity. The machining induced damage in the CD coupons began to propagate under cyclic loading during the early stages after this threshold, whereas delamination did not initiate and propagate for the AWJ coupons until much later. Recall that the hole surface roughness values for the CD coupons were lower than the AWJ coupons, thus these results support the finding that surface roughness alone is not a good indicator of hole quality. This is an important finding for understanding the long-term fatigue performance of fabric-reinforced polymer composites materials with machined holes.

5. Conclusions

A study was conducted in order to investigate the influence of conventional drilling (CD) and abrasive water jet (AWJ) machining processes on the tensile static and fatigue performance of two composite plates with round holes: five harness satin and eight harness satin woven carbon fiber/epoxy. The results of this study provide data that is currently lacking in the literature for fabric-reinforced polymer composites, as well as important qualitative observations for the

corresponding manufacturing induced damage modes and the hole surface roughness. The presented results are also crucial for designing and assessing the long-term performance of practical composite structures manufactured from these materials, specifically those that require mechanical assembly of different components containing holes. Although the plates with AWJ holes exhibited greater long-term fatigue performance at high stress levels for both material systems, which is one of the key findings of this study, the static strength, endurance limit and short-term fatigue behaviour were not influenced by the hole machining process. A second key finding of this study was that the measured hole surface roughness alone is not a good indicator of machined hole quality, and that an investigation of the damage depth penetration into the material from the hole surface is necessary. These findings are contrary to previously reported work on multidirectional laminates, and may be attributed to lower notch sensitivity and fiber architecture of the fabric-reinforced composites. Also, if greater long-term performance is an important design criterion, it should be noted that the component shape may constrain the feasibility of using an AWJ hole drilling process. However, an advantage with the AWJ process is that there is no tool wear, which for drilling operations can lead to deteriorating hole quality as the bit wears. These important points should be considered if AWJ processes are used to machine holes in fabric carbon fiber/epoxy components. Accordingly, the results of this study provide an important cautionary note against the wholesale assessment, often seen in similar studies, of the merit of one of the two machining processes over the other. Indeed, as the results clearly indicate, only after careful consideration of the loading nature (static vs. cyclic) and magnitude of the cyclic loads (low, intermediate or high) can one draw any conclusions about which of the two processes is superior.

Future work will include studying different materials systems, such as braided CFRPs and fabric reinforced GFRPs, in order to determine if the exhibited material behaviour is characteristic of all fabric-reinforced polymer composites. Furthermore, the effects of tool wear and tool geometry on the drilled hole surface quality will also be investigated, as these factors can influence drilling-induced damage. For example, it is known that certain drill bit geometries can act to reduce the severity of exit plane delamination, however, their effect on the development of other damage modes for fabric CFRPs is not clear. Finally, the influence of plate thickness and hole diameter for both drilling methods considered may also be studied, as these variables may also impact hole quality and performance.

Acknowledgements

The authors acknowledge financial support from the Natural Sciences and Engineering Research Council of Canada (NSERC).

References

1. Bannister MK. Development and application of advanced textile composites. Proc Inst Mech Eng Part L - J Mater Des Appl 2014;**218**:253-260.
2. Persson E, Eriksson I, Zackrisson L. Effects of hole machining defects on strength and fatigue life of composite laminates. Compos Part A. 1997;**28**:141-51.
3. Bi ZM, Hinds B, Lin Y, Gibson R, McToal P. Studies on composite drilling – the state of the art. In: Davim JP (ed) Drilling of composite materials, pp 137-73. Nova Science Publisher, New York; 2009.
4. Antoniomaria DL, Alfonso P, Francesco V. Tool wear in drilling thermoset and thermoplastic matrix composites. Eng Syst Des Anal 1996;**75**:41-46.
5. Dharan CKH, Won MS. Machining parameters for an intelligent machining system for composite laminates. Int J Mach Tools Manuf 2000;**40**:415-426.
6. Langella A, Nele L, Maio A. A torque thrust prediction model for drilling of composite materials. Compos Part A 2005;**36**:83-93.
7. Mohan NS, Ramachandra A, Kulkarni SM. Machining of fiber-reinforced thermoplastics: Influence of feed and drill size on thrust force and torque during drilling. J Reinf Plast Compos 2005;**24**:1247-1257.

8. Davim JP, Campos Rubio J, Abrao AM. A novel approach based on digital image analysis to evaluate delamination factor after drilling composite laminates. Compos Sci Technol 2007;**67**:1939-1945.
9. Singh I, Bhatnagar N, Viswanath P. Drilling of uni-directional glass fiber reinforced plastics - experimental & finite element studies. J Mater Des 2008;**29**:546-553.
10. Manna A, Mohindra V, Patra S, Salodkar SM. Drilling of e-glass fibre reinforced polymer composite. Int J Mach Mach Mater 2008;**3**:343-355.
11. Faria PE, Campos Rubio JC, Abrao AM, Davim JP. Dimensional and geometric deviations induced by drilling of polymeric composite. J Reinf Plast Compos 2009;**28**:2535-2363.
12. Kilickap E. Optimization of cutting parameters on delamination based on Taguchi method during drilling of GFRP composite. Exp Syst Appl 2010:**37**:6116-6122.
13. Kilickap E. Investigation into the effect of drilling parameters on delamination in drilling GFRP. J Reinf Plast Compos 2010;**29**:3498-3503.
14. Cong WL, Pei ZJ, Deines TW, Treadwell C. Rotary ultrasonic machining of CFRP using cold air as coolant: Feasibility regions. J Reinf Plast Compos 2011:**30**:899-906.
15. Latha B, Senthilkumar VS, Palanikumar K. Influence of drill geometry on thrust force in drilling GFRP composites. J Reinf Plast Compos 2011;**30**:463-472.
16. Isbilir O, Ghassemieh E. Delamination and wear in drilling of carbon-fiber reinforced plastic composites using multilayer TiAlN/TiN PVD-coated tungsten carbide tools. J Reinf Plast Compos 2012;**31**:717-727.
17. Khan ZM, Mahmood AH, Mills B, Khan LA. The drilling-induced failure mechanisms in T800/924C toughened carbon-epoxy composite materials. J Reinf Plast Compos 2013;**33**:202-211.
18. Catche S, Piquet R, Lachaud F, Castanie B, Benaben A. Analysis of hole wall defects of drilled carbon fiber reinforced polymer laminates. J Compos Mater 2014;**49**:1223-40.
19. Feito N, Diaz-Alvarez A, et al. Experimental analysis of special tool geometries when drilling woven and multidirectional CFRPs. J Reinf Plast Compos 2015;**35**:33-55.
20. Durao LMP, Tavares JMRS, De Albuquerque VHC, Marques JFS, Andrade ONG. Drilling damage in composite material. Materials 2014;**7**:3802-19.
21. Isbilir O, Ghassemieh E. Finite element analysis of drilling of carbon fiber reinforced composites. Appl Compos Mater 2012;**19**:637-656.
22. Khashaba UA. Delamination in drilling polymeric composites: a review. In: Davim JP (ed) Drilling of composite materials, pp 57-81. Nova Science Publisher, New York; 2009.
23. Khashaba UA, El-Sonbaty IA, Selmy AI, Megahed AA. Machinability analysis in drilling woven GFR epoxy composites: part I - effect of machining parameters. Compos Part A 2010;**41**:391-400.
24. Saleem M, Toubal L, Zitoune R, Bougherara H. Investigating the effect of machining processes on the mechanical behavior of composite plates with circular holes. Compos Part A 2013;**55**:169-177.
25. Azmir MA, Ahsan AK. Investigation on glass/epoxy composite surfaces machined by abrasive water jet machining. J Mater Proces Technol 2008;**198**:122-128.
26. Ramulu M, Hwang I, Isvilanonda V. Quality issues associated with abrasive waterjet cutting and drilling of advanced composites. In: American Water Jet Technology Association Conference and Expo, Houston, US, 18-20 August, 2009.

27. Haddad M, Zitoune R, Bougherara H, Eyma F, Castanie B. Study of trimming damages of CFRP structures in function of the machining processes and their impact on the mechanical behaviour. Compos Part B 2014;**57**:136-143.
28. Haddad M, Zitoune R, Eyma F, Castanie B. Influence of machining process and machining induced surface roughness on mechanical properties of continuous fiber composites. Exp Mech 2015;**55**:519-528.
29. Saoudi J, Zitoune R, Mezlini S, Gururaja S, Seitier P. Critical thrust force predictions during drilling: analytical modeling and x-ray tomography quantification. Compos Struct 2016;**153**:886-894.
30. Ibraheem HMA, Iqbal A, Hashemipour M. Numerical optimization of hole making in GFRP composite using abrasive water jet machining. J Chinese Inst Eng 2015;**38**:66-76.
31. Hashish M, Steele DE, Bothell DH. Machining with super-pressure (690 MPa) waterjets. Int J Mach Tools Manuf 1997;**37**:465-479.
32. Bhattacharyya D, Horrigan DPW. A study of hole drilling in kevlar composites. Compos Sci Technol 1998;**58**:267-283.
33. Ramulu M, Wern CW, Garbini JL. Effect of fiber direction on surface roughness of machined graphite/epoxy composite. Compos Manuf 1993;**4**:39-51.
34. Saleem M. A non-destructive study of a carbon fibre epoxy composite plate using lock-in thermography, cyclic loading, and finite element analysis. MASc Thesis, Ryerson University, Canada; 2010.
35. Montesano J, Fawaz Z, Bougherara H. Use of infrared thermography to investigate the fatigue behaviour of a carbon fiber reinforced polymer composite. Compos Struct 2013;**97**:76-83.
36. LaRosa G, Risitano A. Thermographic methodology for rapid determination of the fatigue limit of materials and mechanical components. Int J Fatigue 2000;**22**:65-73.
37. Avdelidis NP, Almond DP, Dobbinson A, Hawtin BC, Ibarra-Castanedo C, Maldague X. Aircraft composites assessment by means of transient thermal NDT. Progress Aero Sci 2004;**40**:143-162.
38. Montesano J, Fawaz Z, Bougherara H. Non-destructive assessment of the fatigue strength and damage progression of satin woven fiber reinforced polymer matrix composites. Compos Part B 2015;**71**:122-130.

Tables

Table 1 CFRP test coupon description

Test Coupon	Material	Hole Machining Method
5HS-CD	5HS	Drilled
8HS-CD	8HS	Drilled
5HS-AWJ	5HS	Water Jet
8HS-AWJ	8HS	Water Jet

Table 2 AWJ and CD average hole surface roughness values for 5HS and 8HS materials

Test Coupon	*Ra* (μm)	*Rq* (μm)	*Rz* (μm)
5HS-CD	1.34	1.73	8.38
8HS-CD	1.16	1.32	6.81
5HS-AWJ	1.95	2.48	10.25
8HS-AWJ	1.85	2.51	10.31

Figures

Fig. 1 (a) Test coupon geometry showing hole size/location and end tabs, and (b) experimental setup using infrared camera showing temperature evaluation zone.

Fig. 2 SEM images of 5HS CFRP plate hole surface (a) AWJ, (b) CD.

Fig. 3 Thermographs captured using pulse thermography technique at test coupon exit plane side showing damage regions around holes for (a) 8HS-AWJ, (b) 8HS-CD.

Fig. 4 Stress-strain curves obtained during ultimate static tests.

Fig. 5 Single test coupon characteristic bilinear temperature-stress data for stepwise cyclic tests (a) 5HS-AWJ, (b) 5HS-CD.

Fig. 6 Single test coupon characteristic bilinear temperature-stress data for stepwise cyclic tests (a) 8HS-AWJ, (b) 8HS-CD.

Fig. 7 Stepwise cyclic test data profiles for AWJ and CD coupons, (a) 5HS woven CFRP normalized stiffness, (b) 5HS woven CFRP temperature rise, (c) 8HS woven CFRP normalized stiffness, (d) 8HS woven CFRP temperature rise.

Fig. 8 Conventional fatigue test data profiles for 8HS-AWJ and 8HS-CD test coupons cycled under a maximum stress of 530 MPa (a) normalized stiffness, (b) temperature rise.

Fig. 9 Thermographs captured using pulse thermography technique at test coupon exit plane side showing damage regions around holes after 150,000 loading cycles (385 MPa) for (a) 5HS-AWJ, (b) 5HS-CD.

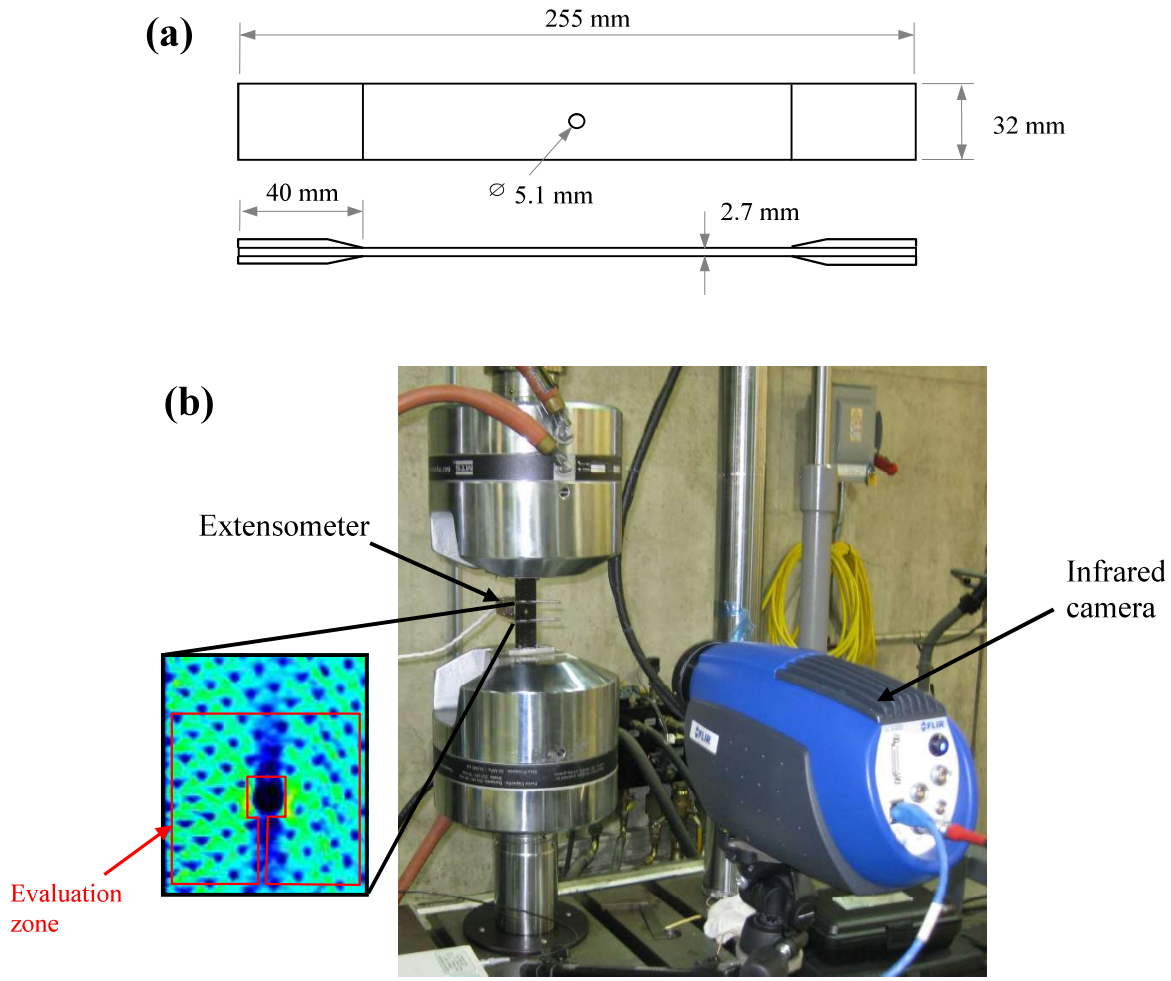
(a)
255 mm
32 mm
∅ 5.1 mm
40 mm
2.7 mm
(b)
Extensometer
Infrared camera
Evaluation zone

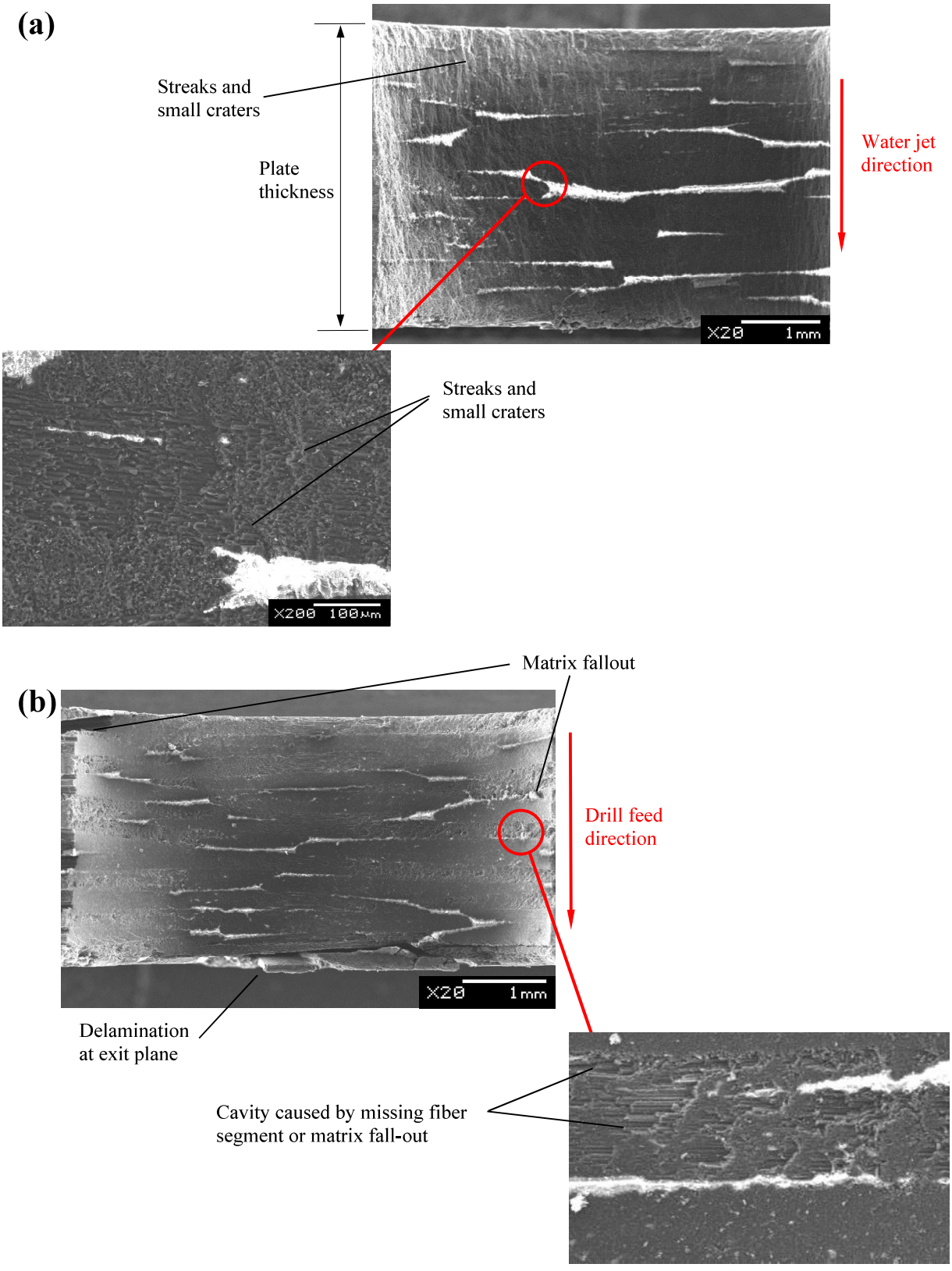
(a)
Streaks and
small craters
Plate
thickness
Water jet
direction
X20 1mm
Streaks and
small craters
X200 100µm
(b)
Matrix fallout
Drill feed
direction
X20 1mm
Delamination
at exit plane
Cavity caused by missing fiber
segment or matrix fall-out

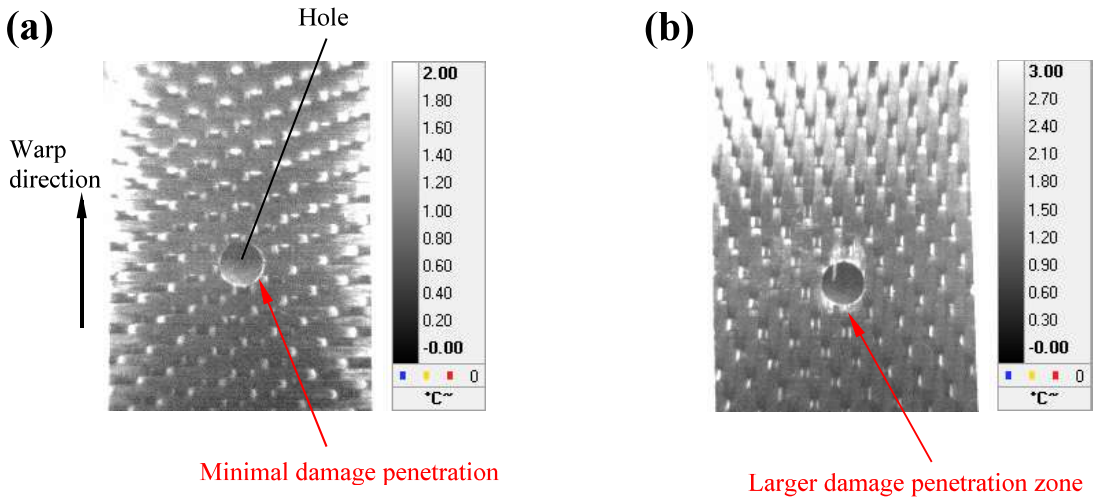
(a)
Hole
Warp direction
2.00
1.80
1.60
1.40
1.20
1.00
0.80
0.60
0.40
0.20
-0.00
°C
Minimal damage penetration
(b)
3.00
2.70
2.40
2.10
1.80
1.50
1.20
0.90
0.60
0.30
-0.00
°C
Larger damage penetration zone

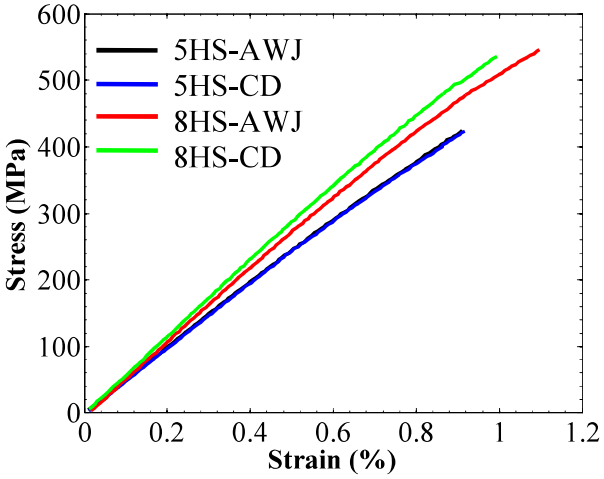
600
500
400
300
200
100
0
Stress (MPa)
0
0.2
0.4
0.6
0.8
1
1.2
Strain (%)
5HS-AWJ
5HS-CD
8HS-AWJ
8HS-CD

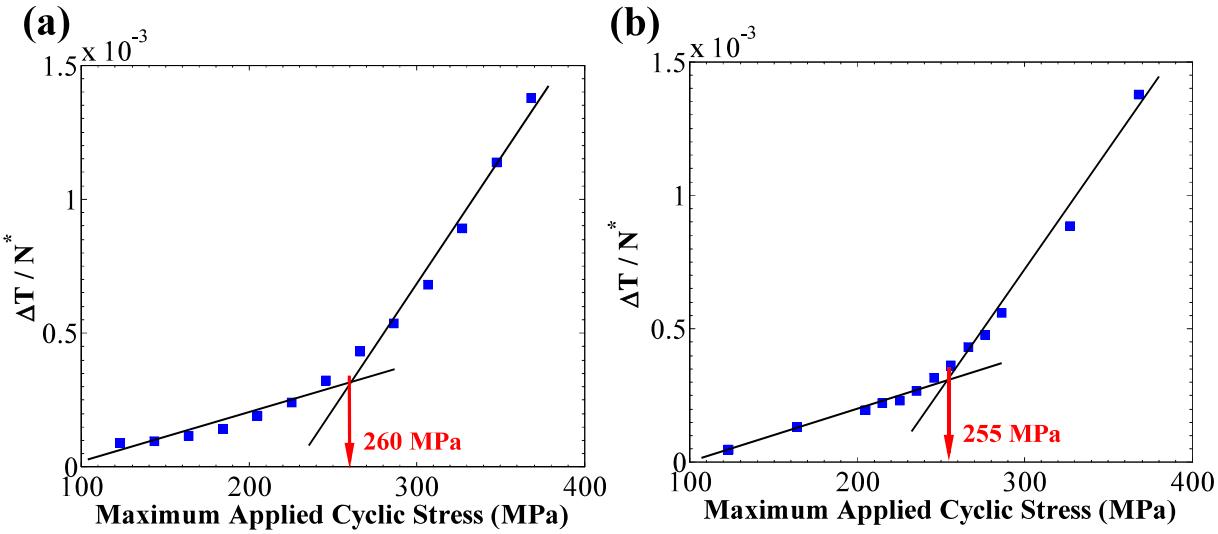
(a)
x 10^-3
1.5
1
0.5
0
ΔT / N*
260 MPa
100
200
300
400
Maximum Applied Cyclic Stress (MPa)
(b)
x 10^-3
1.5
1
0.5
0
ΔT / N*
255 MPa
100
200
300
400
Maximum Applied Cyclic Stress (MPa)

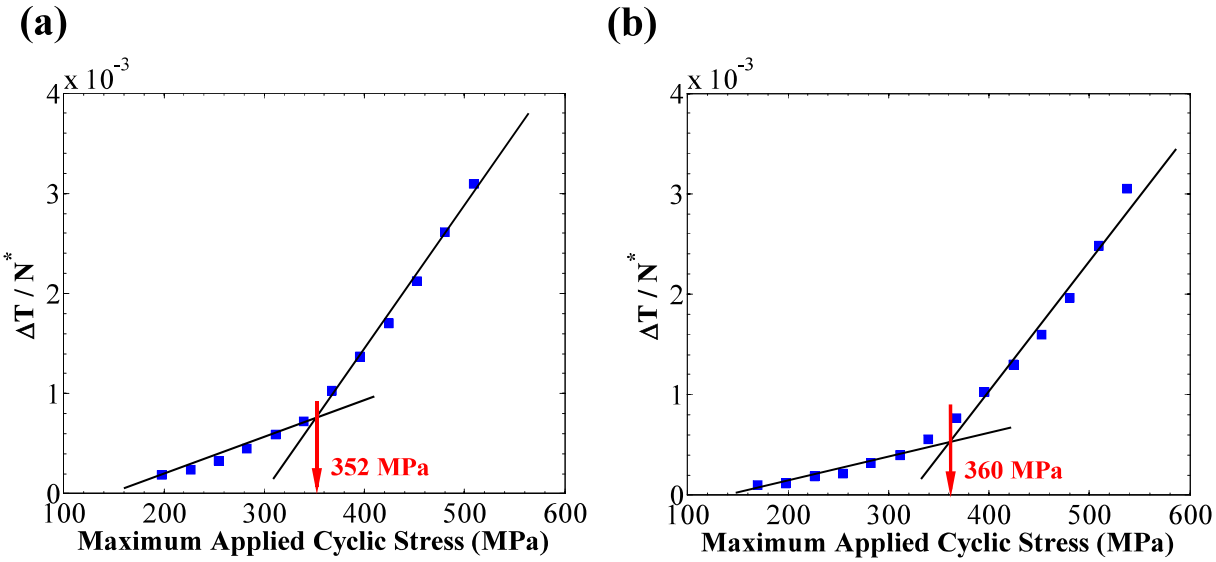
(a)
x 10^-3
4
3
2
1
0
ΔT / N*
352 MPa
100
200
300
400
500
600
Maximum Applied Cyclic Stress (MPa)
(b)
x 10^-3
4
3
2
1
0
ΔT / N*
360 MPa
100
200
300
400
500
600
Maximum Applied Cyclic Stress (MPa)

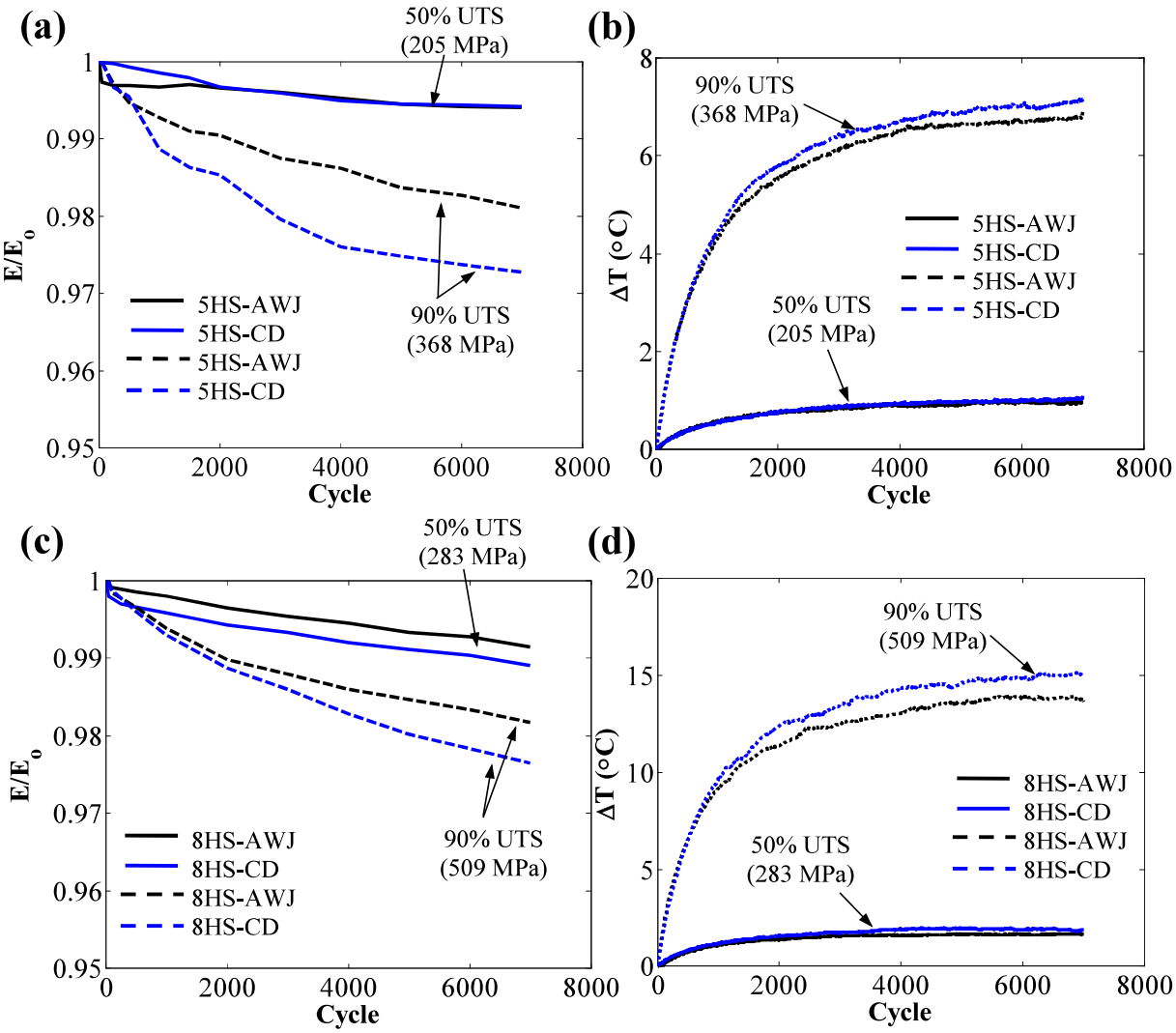
(a)
50% UTS
(205 MPa)
90% UTS
(368 MPa)
5HS-AWJ
5HS-CD
5HS-AWJ
5HS-CD
E/E$_o$
Cycle
(b)
90% UTS
(368 MPa)
50% UTS
(205 MPa)
5HS-AWJ
5HS-CD
5HS-AWJ
5HS-CD
ΔT (°C)
Cycle
(c)
50% UTS
(283 MPa)
90% UTS
(509 MPa)
8HS-AWJ
8HS-CD
8HS-AWJ
8HS-CD
E/E$_o$
Cycle
(d)
90% UTS
(509 MPa)
50% UTS
(283 MPa)
8HS-AWJ
8HS-CD
8HS-AWJ
8HS-CD
ΔT (°C)
Cycle

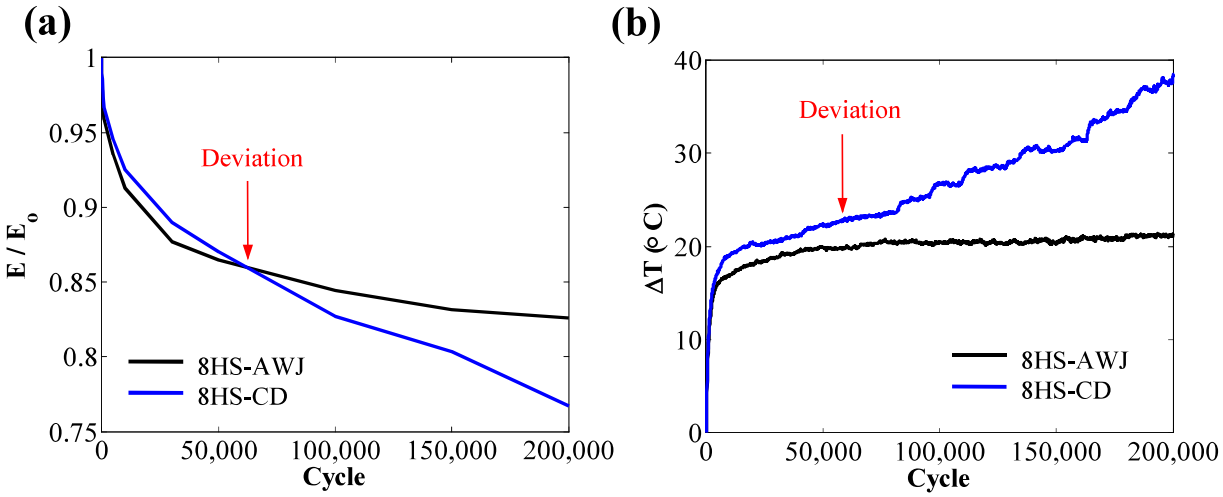
(a)
1
0.95
0.9
0.85
0.8
0.75
E / E_o
Deviation
8HS-AWJ
8HS-CD
0
50,000
100,000
150,000
200,000
Cycle
(b)
40
30
20
10
0
ΔT (°C)
Deviation
8HS-AWJ
8HS-CD
0
50,000
100,000
150,000
200,000
Cycle

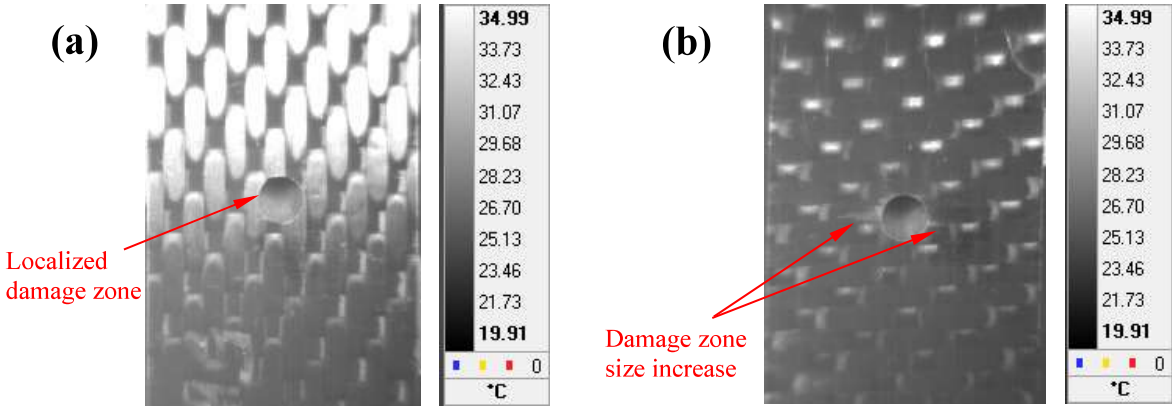
(a)
Localized
damage zone
34.99
33.73
32.43
31.07
29.68
28.23
26.70
25.13
23.46
21.73
19.91
0
°C
(b)
Damage zone
size increase
34.99
33.73
32.43
31.07
29.68
28.23
26.70
25.13
23.46
21.73
19.91
0
°C